

Article

Critical Assessment of the Effect of Atmospheric Corrosion Induced Hydrogen on Mechanical Properties of Advanced High Strength Steel

Darya Rudomilova ^{1,*}, Tomáš Prošek ¹ , Ines Traxler ², Josef Faderl ³, Gerald Luckeneder ³, Gabriela Schimo-Aichhorn ² and Andreas Muhr ³

- ¹ Technopark Kralupy, University of Chemistry and Technology Prague, 166 28 Prague, Czech Republic; tomas.prosek@vscht.cz
- ² CEST Kompetenzzentrum für Elektrochemische Oberflächentechnologie GmbH, 4020 Linz, Austria; ines.traxler@cest.at (I.T.); gabriela.schimo@cest.at (G.S.-A.)
- ³ Voestalpine Stahl, 4020 Linz, Austria; Josef.Faderl@voestalpine.com (J.F.); Gerald.Luckeneder@voestalpine.com (G.L.); Andreas.Muhr@voestalpine.com (A.M.)
- * Correspondence: darya.rudomilova@vscht.cz; Tel.: +420-220-446-134

Abstract: Hydrogen absorption into steel during atmospheric corrosion has been of a strong concern during last decades. It is technically important to investigate if hydrogen absorbed under atmospheric exposure conditions can significantly affect mechanical properties of steels. The present work studies changes of mechanical properties of dual phase (DP) advanced high strength steel specimens with sodium chloride deposits during corrosion in humid air using Slow Strain Rate Test (SSRT). Additional annealed specimens were used as reference in order to separate the possible effect of absorbed hydrogen from that of corrosion deterioration. Hydrogen entry was monitored in parallel experiments using hydrogen electric resistance sensor (HERS) and thermal desorption mass spectrometry (TDMS). SSRT results showed a drop in elongation and tensile strength by 42% and 6%, respectively, in 27 days of atmospheric exposure. However, this decrease cannot be attributed to the effect of absorbed hydrogen despite the increase in hydrogen content with time of exposure. Cross-cut analysis revealed considerable pitting, which was suggested to be the main reason for the degradation of mechanical properties.

Keywords: high strength steels; hydrogen embrittlement; atmospheric corrosion; slow strain rate test



Citation: Rudomilova, D.; Prošek, T.; Traxler, I.; Faderl, J.; Luckeneder, G.; Schimo-Aichhorn, G.; Muhr, A. Critical Assessment of the Effect of Atmospheric Corrosion Induced Hydrogen on Mechanical Properties of Advanced High Strength Steel. *Metals* **2021**, *11*, 44. <https://dx.doi.org/10.3390/met11010044>

Received: 9 December 2020

Accepted: 23 December 2020

Published: 28 December 2020

Publisher's Note: MDPI stays neutral with regard to jurisdictional claims in published maps and institutional affiliations.



Copyright: © 2020 by the authors. Licensee MDPI, Basel, Switzerland. This article is an open access article distributed under the terms and conditions of the Creative Commons Attribution (CC BY) license (<https://creativecommons.org/licenses/by/4.0/>).

1. Introduction

Hydrogen embrittlement of advanced high strength steels (AHSSs) in atmospheric exposure conditions is of high importance for automotive industry as the application of AHSSs grows steadily due to their desirable mechanical properties. Combination of soft and hard phases in the AHSS microstructure allows for maintaining good ductility with increased tensile strength [1–4]. Dual-phase (DP) steels microstructure consists of hard martensite islands in a soft ferrite matrix. In automotive industry, DP AHSSs are used in various car component such as pillars, door beams, side members, body reinforcements and their applications continue to expand [3].

Different aspects of the hydrogen embrittlement phenomenon such as hydrogen entry caused by atmospheric corrosion reactions are currently under intensive research. One of the important issues is an assessment of risk of brittle fracture caused by hydrogen under service conditions. The principal question is if a very small amount of hydrogen entering steel because of atmospheric corrosion might cause any significant change of mechanical properties.

Hydrogen embrittlement susceptibility can be assessed by the slow strain rate test (SSRT) [5]. During SSRT, applied stress is gradually increased and hydrogen simultaneously

accumulates in the stress field [6,7]. SSRT has been performed after electrochemical pre-charging [8–13], during electrochemical in situ charging [14–17], immersion in solutions [18] and in gaseous hydrogen atmosphere [19,20]. Few authors tested mechanical properties of AHSSs after outdoor exposures or cyclic corrosion testing [21,22]. There is obviously still a lack of reports about fracture behavior of AHSSs under atmospheric corrosion conditions.

Diffusible atomic hydrogen is responsible for loss of ductility of AHSSs during straining caused by hydrogen accumulation near dislocation sites and microvoids [17]. Hydrogen can interact with dislocations causing their enhanced mobility, which alternates the fracture behavior [23,24]. The critical hydrogen content can be used to indicate the dangerous hydrogen level causing a significant loss of mechanical properties [8,25]. However, reported values of critical hydrogen contents differ strongly. For example, values such as 4 ppm for vanadium-bearing high strength steel [26]; 0.64 ppm and 1 ppm for 2.25Cr-1Mo steel [15]; or 0.5 ppm for SCM435 steel [8] have been reported. Li et al. [22] defined 0.04, 0.25 and 0.58 ppm for AISI 4135 with tensile strengths of 1300 and 1500 MPa and boron-bearing steel with 1300 MPa, respectively, as minimum hydrogen contents needed to cause brittle fracture. Thus, the critical hydrogen content is a material-dependent parameter. This critical value is usually evaluated quantitatively using thermal desorption spectroscopy (TDS) or thermal desorption mass spectrometry (TDMS), where hydrogen desorption flux is measured under controlled temperature ramping conditions. Hydrogen quantification is conducted using gas chromatography or mass spectrometry. Disadvantage of these techniques is that they neglects mobile hydrogen, which cannot be measured ex situ due to high hydrogen lattice diffusion rates [27,28]. However, all diffusible hydrogen atoms, both reversibly trapped and mobile, may be driven into regions with high stress and play a role in crack propagation [17]. In situ hydrogen monitoring allows detection of mobile hydrogen entering steel during atmospheric corrosion. It was shown that a hydrogen electric resistance sensor (HERS) may be used for such in situ detection of hydrogen diffusing through a corroding specimen [27]. The amount of hydrogen passing through the sample is monitored via changes of electric resistance of a hydrogen probe (H-probe) made of V-Nb-Ta alloy [29].

In summary, it has been proved repeatedly that AHSS are susceptible to hydrogen embrittlement when charged with a sufficiently high amount of atomic hydrogen [6,7,9,30–34]. It was also shown that atomic hydrogen can enter AHSS under atmospheric exposure conditions [35–37]. Now, the technically critical question is whether the amount of hydrogen formed in relevant atmospheric environments on corroding AHSS members is high enough to induce significant loss of mechanical properties. Such data are scarce.

In the current work, the effect of atmospherically induced hydrogen on mechanical properties of AHSSs was assessed in situ by SSRT. In parallel measurements, diffusible hydrogen was monitored in situ using HERS and ex situ with TDMS.

2. Materials and Methods

Dual phase AHSS DP1000 with ultimate tensile strength R_m 980 MPa was used in this work [38]. The chemical composition of the steel is given in Table 1. The DP1000 steel microstructure consists of 36% of ferrite phase and 64% of martensite phase [39]. The scanning electron microscope (SEM) image of the DP1000 microstructure is shown in Figure 1. The thickness of steel sheet was 0.81 ± 0.01 mm.

Table 1. Chemical composition of AHSS; maximal concentrations of elements in wt.%.

Material/Element	C	Mn	P	S	Si	Al	Cr + Mo	Nb + Ti	B	V
DP1000	0.18	2.5	0.08	0.015	0.8	2.0	1.4	0.15	0.005	0.2

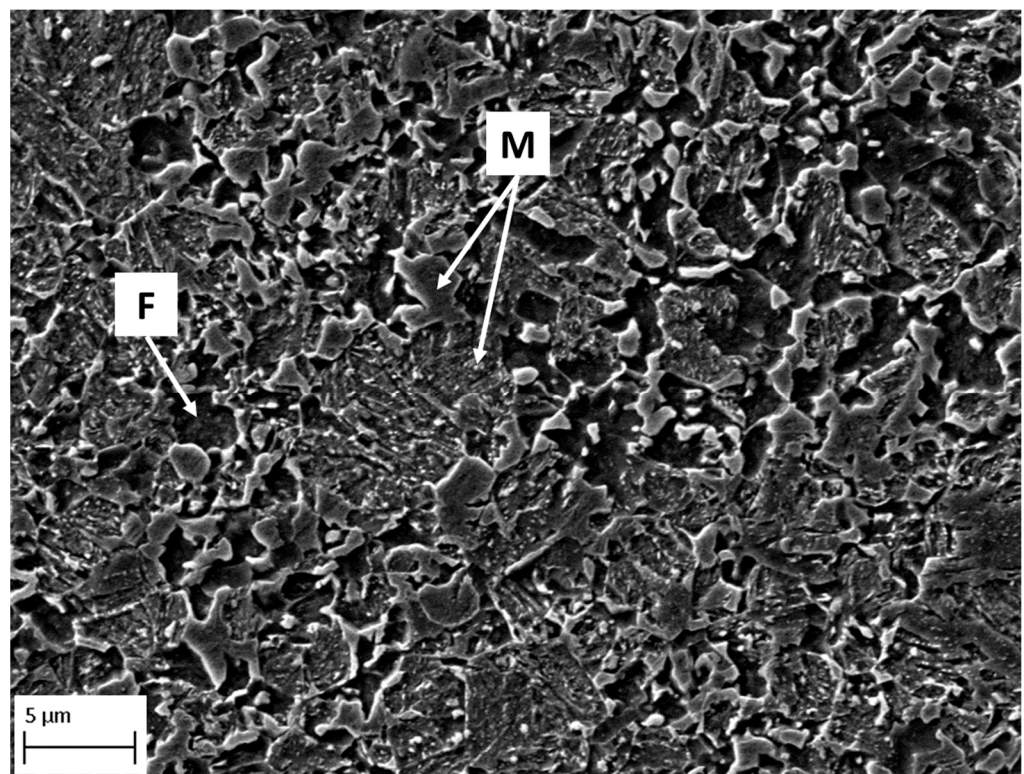


Figure 1. Microstructure of DP1000 from SEM after etching; F—ferrite, M—martensite.

HERS was used for in situ monitoring of the added diffusible hydrogen content. The HERS (KircTec GmbH, Göttingen, Germany) is a device for hydrogen permeation measurements based on monitoring electric resistance changes [27]. An uncoated DP1000 specimen was polished and degreased in acetone on both sides. An H-probe was welded to one side of the specimen denoted as *H exit side*. On the opposite *H entry side*, 330 μL of 0.1 M NaCl methanol solution was applied to an area of 12.25 cm^2 . After methanol evaporation in a stream of warm air, a uniform layer of NaCl deposits with the surface chloride concentration of 100 $\mu\text{g}\cdot\text{cm}^{-2}$ (1 $\text{g}\cdot\text{m}^{-2}$) was obtained [40]. Deposits with a similar composition were reported to form on metallic structures in coastal regions or in a vicinity of roads where de-icing salts are used in a range of days to months [41,42]. The samples were exposed to air at constant relative humidity (RH) of 85% in a climatic chamber with controlled temperature of 25 $^{\circ}\text{C}$. The RH level was chosen based on results of preliminary experiments showing enhanced hydrogen absorption at 85% RH.

For comparison, the added diffusible hydrogen content was determined also ex situ using TDMS after different exposure durations. NaCl solution was deposited on steel samples using the procedure described above to obtain the surface chloride concentration of 100 $\mu\text{g}\cdot\text{cm}^{-2}$ (1 $\text{g}\cdot\text{m}^{-2}$). The samples were exposed to air at constant RH of 85%. Prior to TDMS, corrosion products were removed by chemical cleaning in HCl 1:1 solution with 4.5 $\text{g}\cdot\text{L}^{-1}$ hexamethylenetetramine as inhibitor. Hydrogen content was measured using Galileo G8 Hydrogen Analyzer (Bruker Elemental GmbH, Kalkar, Germany) coupled to a customized GAM200 quadrupole mass spectrometer (InProcess Instruments Gesellschaft für Prozessanalytik mbH, Bremen, Germany). The isothermal measurement at 350 $^{\circ}\text{C}$ was conducted in order to obtain the hydrogen content.

It should be noted that although the diffusible hydrogen content in as-received DP1000 is low, some residual hydrogen can still be present in the steel structure. Our TDMS measurements showed there were up to 0.1 ppm diffusible hydrogen in the as-received samples. Since this work focuses on hydrogen absorbed during atmospheric exposure experiments, the residual hydrogen content was deduced from both HERS and TDMS

data and the *added diffusible hydrogen content* is reported. For sake of simplicity, this term is shortened to the *hydrogen content* in the following text.

The effect of hydrogen on mechanical properties of DP1000 was studied using SSRT. Tensile test specimens with the gauge length of 33 mm were machined from steel sheets using water jet cutter. Their geometry is illustrated in Figure 2. The specimens were annealed at 200 °C for 2 h in order to remove hydrogen eventually introduced during handling and cutting. Annealing at 200 °C is considered to be sufficient for mobile hydrogen release [43,44]. Then, NaCl solution was deposited all over the gauge length to obtain the surface chloride concentration of $100 \mu\text{g}\cdot\text{cm}^{-2}$ ($1 \text{ g}\cdot\text{m}^{-2}$) and the specimens were pre-exposed to air at 85% RH and at laboratory temperature of 21–23 °C. There were two groups of specimens. The specimens denoted as *Corroding* were transferred from the pre-exposure chamber to the chamber attached to the SSRT machine without any intermediate operation. The relative humidity was kept at the same level of 85% in both chambers to ensure continuous hydrogen uptake. The *Annealed* specimens were annealed at 200 °C for 2 h after the pre-exposure in order to remove absorbed hydrogen and the SSRT was conducted in dry air to avoid any further corrosion and hydrogen entry. The *Annealed* specimens were used as reference in order to separate the possible effect of absorbed hydrogen from that of corrosion deterioration on mechanical properties. Slow strain rate tests were performed at $7\cdot 10^{-4} \text{ mm}\cdot\text{min}^{-1}$ crosshead displacement speed with the initial stress of 100 MPa. Stress-strain curves were measured and tensile strength and elongation were evaluated. Fractographic analysis was performed using a scanning electron microscope (SEM) ZEISS EVO 15 (Carl Zeiss AG, Oberkochen, Germany) with 15 kV accelerating voltage. The fracture geometry was analyzed with a stereo microscope Olympus SZX7 (Olympus, Tokyo, Japan).

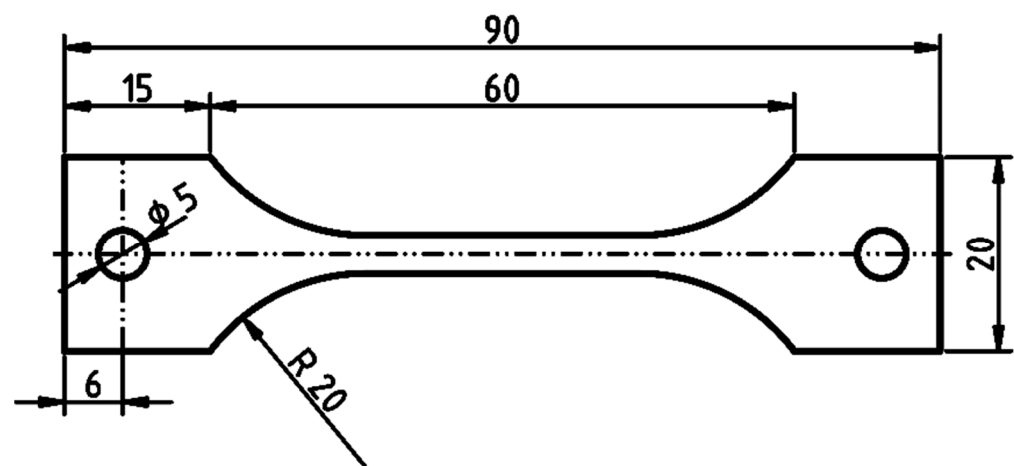


Figure 2. Geometry of tensile specimens; dimensions in mm.

3. Results

3.1. Atmospherically Induced Hydrogen Uptake

Content of the added diffusible hydrogen in a specimen with chloride deposits exposed to humid air was monitored using HERS. During first 2 days, the specimen was exposed to dry conditions at 4% RH to get stable signal reading. Then, the relative humidity was increased to 85% and maintained constant until end of the experiment. Figure 3 shows evolution of the hydrogen content with time of exposure from the start of the humid phase. Hydrogen content started to grow 5 days after introduction of humid air. This time lag can be attributed to the time needed for formation of rust layer and development of localized corrosion, as the process of hydrogen adsorption is related to the localized anodic sites underneath red rust [45]. The hydrogen content grew at a constant rate of $0.03\text{--}0.04 \text{ ppm}\cdot\text{day}^{-1}$. It started to stabilize after 33 days of exposure at about 1.1–1.2 ppm. Akiyama et al. [46] noticed that hydrogen content becomes independent of the exposure

time after an initial increase. The plateau was observed after 60 8-h cycles of exposure in corrosive environment on samples with pre-deposited NaCl [36] or after 30 cycles of salt spray phases [47]. The plateau level of diffusible hydrogen measured with TDMS was about 0.06–0.08 ppm [36,47]. In the current work, static exposure conditions were chosen to maximize the hydrogen content in the sample. It can be assumed that cycling of the RH, typical for real atmospheric exposures, would lead to a lower hydrogen uptake into the investigated steel.

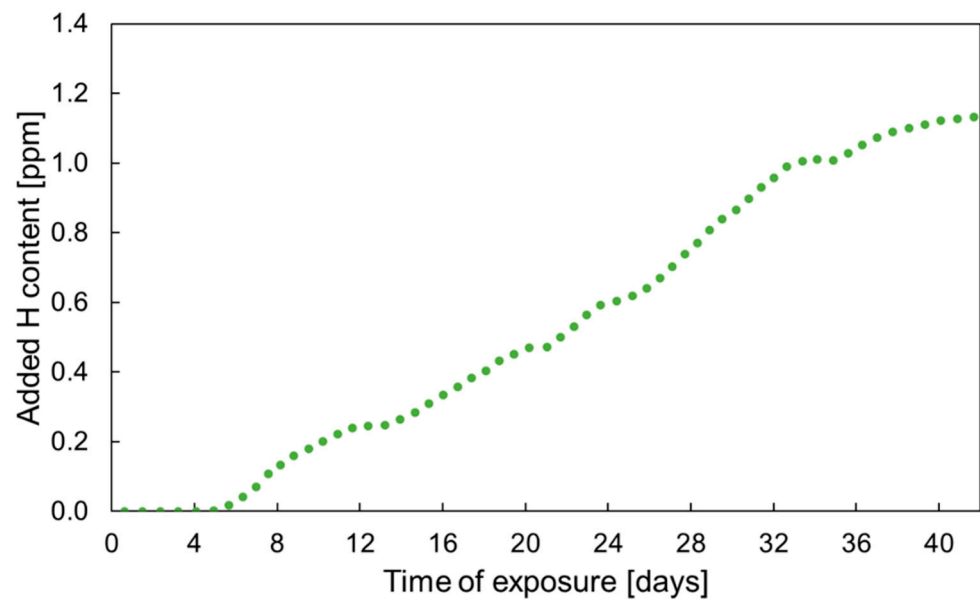


Figure 3. HERS measurement of added diffusible hydrogen content in DP1000 AHSS with NaCl deposits in humid air at 85% RH.

TDMS measurements were conducted on parallel corroded samples in order to confirm the HERS data. Added diffusible hydrogen contents measured by TDMS and HERS are compared in Figure 4 with error bars representing the standard deviation for the TDMS values. Although the data show a scatter between samples especially in the beginning of the exposure, the increase of hydrogen content becomes obvious after 5 days of exposure. The TDMS measurements show reasonably good correlation with HERS results for the same period of time considering natural differences in corrosion processes on parallel samples. Anyway, the data indicate somewhat lower sensitivity of the HERS technique at very low hydrogen concentrations. A new experiment aiming at comparison of longer-term TDMS and HERS data is in progress.

It can be noticed that the TDMS data obtained in the beginning of the exposure show quite large scatter. This can be due to more pronounced initial differences in the corrosion process between individual samples affecting the hydrogen entry.

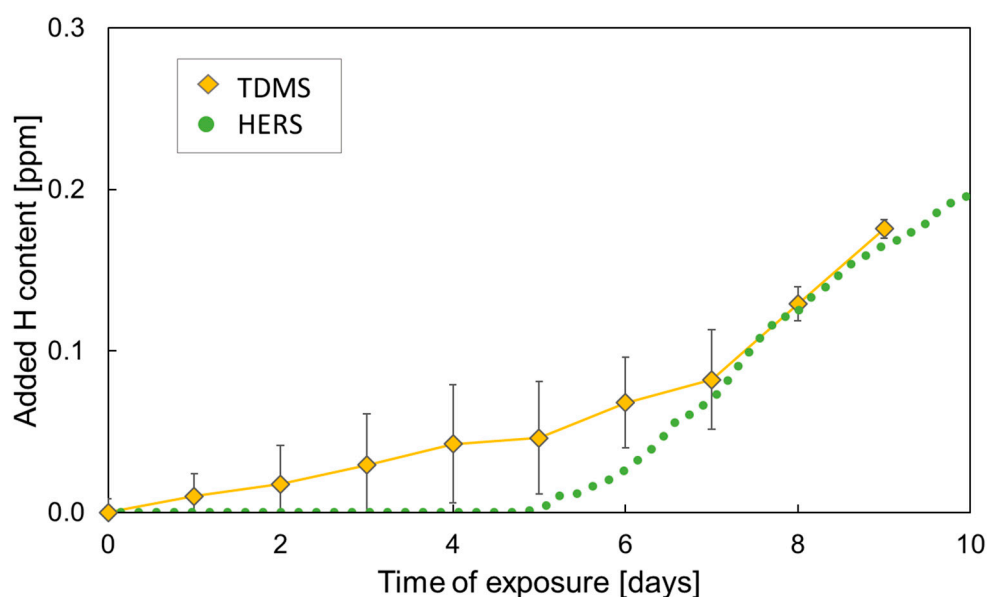


Figure 4. Comparison of TDMS and HERS measurements of added diffusible hydrogen content in DP1000 AHSS with NaCl deposits in humid air at 85% RH.

3.2. Slow Strain Rate Test

To study the effect of hydrogen absorbed under atmospheric corrosion conditions on mechanical properties of AHSS, SSRT was carried out with specimens pre-exposed in air at 85% RH for varying periods of time. Figure 5 presents changes of elongation and tensile strength as a function of exposure time to humid air. Each data point represents an average value for 3 or 4 parallel specimens with error bars giving standard deviations. For the *Corroding* specimens, the time of exposure includes the pre-exposure and the tensile testing period, as the specimens were exposed to humid air during the SSRT. The *Annealed* specimens were exposed to humid conditions only during the pre-exposure period. The trend of a decrease in elongation and tensile strength for the *Corroding* specimens is clearly observed. The elongation decreased by 42% during 27 days of exposure. A less pronounced drop of 6% was recorded for tensile strength. It should be noted that the values of tensile strength were calculated using the initial cross-sectional area of the specimens. Although the cross-sectional area decreased due to corrosion, as discussed in the following sections, the reduction was non-uniform along the specimen's length and could not be estimated correctly.

If only the *Corroding* samples are considered, this observation could be interpreted as the effect of atomic hydrogen. However, for both elongation and tensile strength, the ranges measured for *Corroding* and *Annealed* reference specimens are overlapping. It can be expected that most of hydrogen absorbed during the pre-exposure was removed by annealing from the reference *Annealed* samples and no further hydrogen formed during the SSRT. Thus, this decrease of mechanical properties cannot be attributed to the effect of absorbed hydrogen.

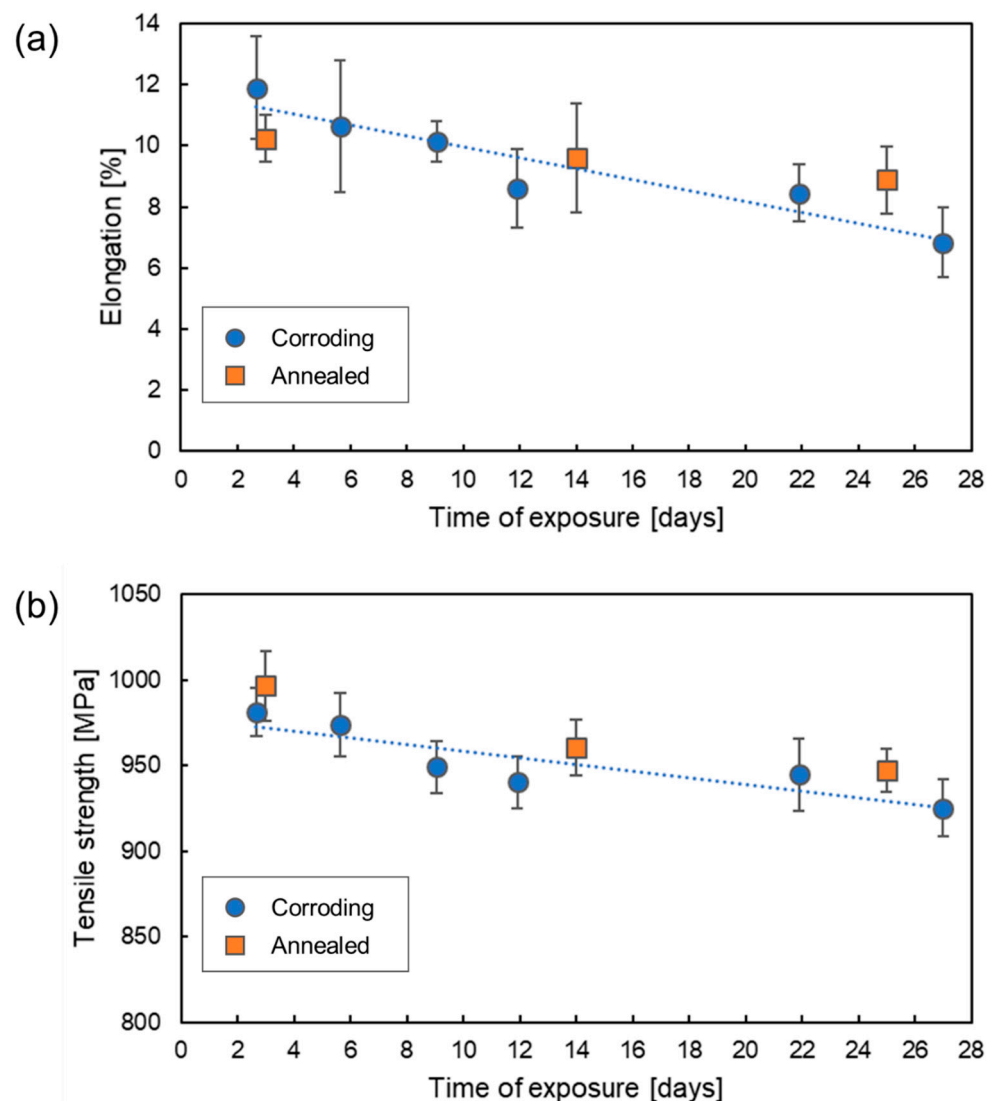


Figure 5. Change in elongation (a) and tensile strength (b) with time of exposure of DP1000 AHSS with NaCl deposits in humid air at 85% RH.

3.3. Fractographic Analysis

Figure 6 illustrates the failure geometry of the selected tensile specimens. All specimens display necking behavior with combination of diffuse and localized necking modes. From the front view, the plain of failure was perpendicular to the tensile axis for almost all specimens, besides few specimens with angled fracture. The lateral slant fracture was found on all specimens indicating ductile fracture mode. The change from ductile to brittle geometry with flat fracture plain is unlikely under conditions used in the current work. Such change was reported for cathodically charged specimens with much higher hydrogen content of 26 and 3 ppm for dual phase and martensitic steel, respectively [48].

Post mortem SEM fractographic analysis showed that fracture surfaces of both *Corroding* and *Annealed* SSRT specimens were entirely dimpled. As an example, Figure 7 shows the fracture surface of a *Corroding* specimen exposed for the longest period of time used in the current work, i.e., 27 days. It should be noted that the change of the fracture mode from ductile to brittle, i.e., formation of quasi-cleavage fracture surfaces with flat facets, can be expected only after more severe hydrogen charging [9,11,17,19,30,49]. Liu and Atrens underlined that ductile dimple fracture can be observed in the presence of low amounts of hydrogen [50].

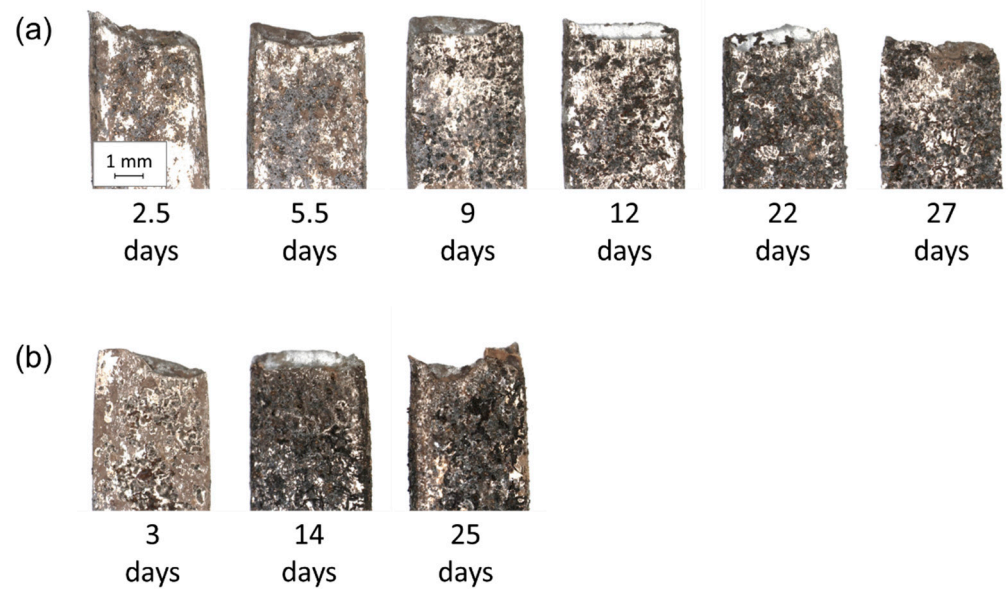


Figure 6. Selected photographs of fractured *Corroding* (a) and *Annealed* (b) tensile specimens exposed in humid air at 85% RH for indicated time.

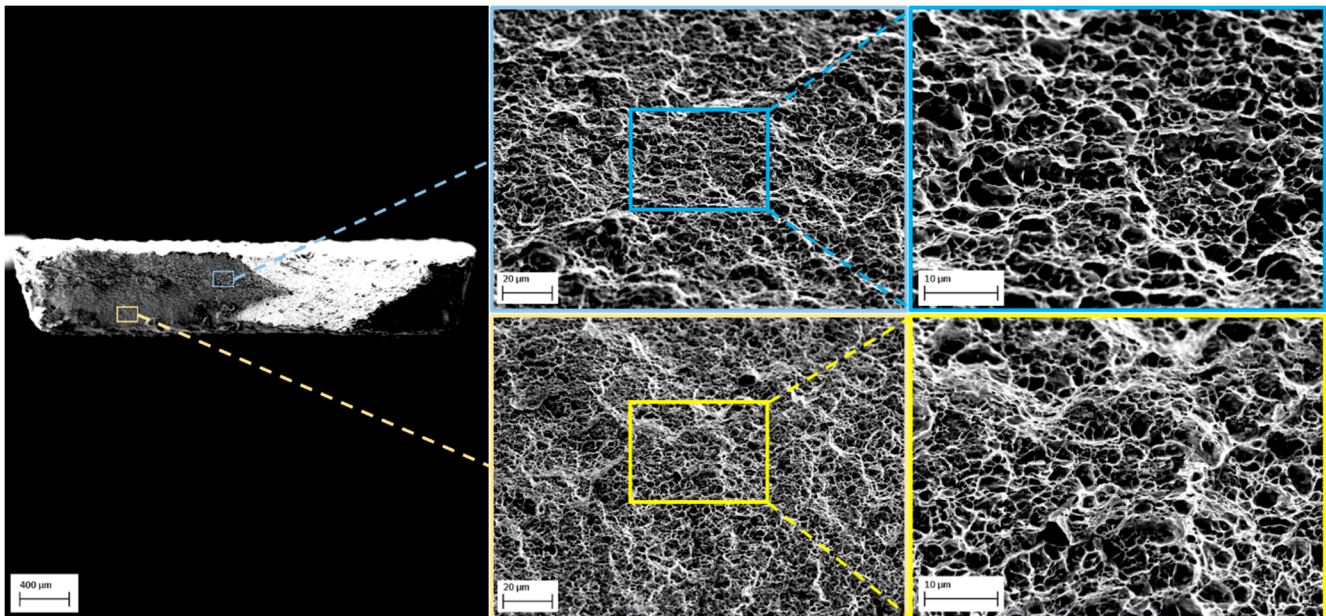


Figure 7. SEM micrographs of fracture surface of DP1000 AHSS *Corroding* specimen with NaCl deposits exposed in humid air at 85% RH for 27 days.

It has been discussed in literature that the dimple morphology may change in presence of relatively low amounts of absorbed hydrogen indicating a change in the fracture behavior. It was claimed that hydrogen can accelerate stages of void nucleation, evolution and coalescence leading to reduction in average dimple size [51–53]. Zhang et al. [51] explained this phenomenon by formation of hydrogen-vacancy complexes. Moreover, formation of fine dimples is in accordance with HELP (Hydrogen-Enhanced Localized Plasticity) and AIDE (Adsorption-Induced Dislocation Emission) mechanisms of hydrogen embrittlement [54]. On the other hand, the increase of the dimple size may be explained by microvoid growth effect. Thus, there is no agreement on the effect of hydrogen on the dimple morphology; the dimples may get smaller, larger or even unchanged in hydrogen-containing specimens [55]. Moreover, the fracture surface of sheet specimens often exhibits regions with different angles, which complicates this quite ambiguous analysis.

Both the fractographic analysis and SSRT data indicate that the amount of hydrogen absorbed during 27 days of the atmospheric exposure was insufficient to cause changes in mechanical properties of the investigated steel. The diffusible hydrogen content measured by HERS in an unstressed specimen was approximately 0.7 ppm after the same exposure period. It can be assumed that the amount of absorbed hydrogen in the SSRT specimens might be even higher as the applied stress probably enhances hydrogen entry. Kushida et al. [56] reported a 3-times higher diffusible hydrogen content in samples under mechanical stress compared to unstressed samples, both corroding under atmospheric exposure. Nevertheless, the amount of hydrogen absorbed under conditions of the current work seems to be insufficient to alter the fracture mechanism.

3.4. Corrosion Morphology

In order to investigate the possible effect of corrosion, cross-sections of the *Corroding* SSRT specimens were analyzed. The fractured SSRT specimens were cross-cut at the same distance from the specimen's edge. The distance between the cross-cut and fracture was about 15–20 mm. Corrosion products were removed using inhibited hydrochloric acid. As examples, cross-sections of specimens exposed for 2.5 and 27 days are shown in Figure 8. Both photographs reveal localized corrosion. Several shallow pits were formed already after 2.5 days of exposure. The longer exposure to the corrosive environment caused a significant increase of the dimples size, see Figure 8b. Even though pitting corrosion is more typical for stainless steel, low-carbon steels might be susceptible to pitting during exposure to chloride-containing environments [57,58].

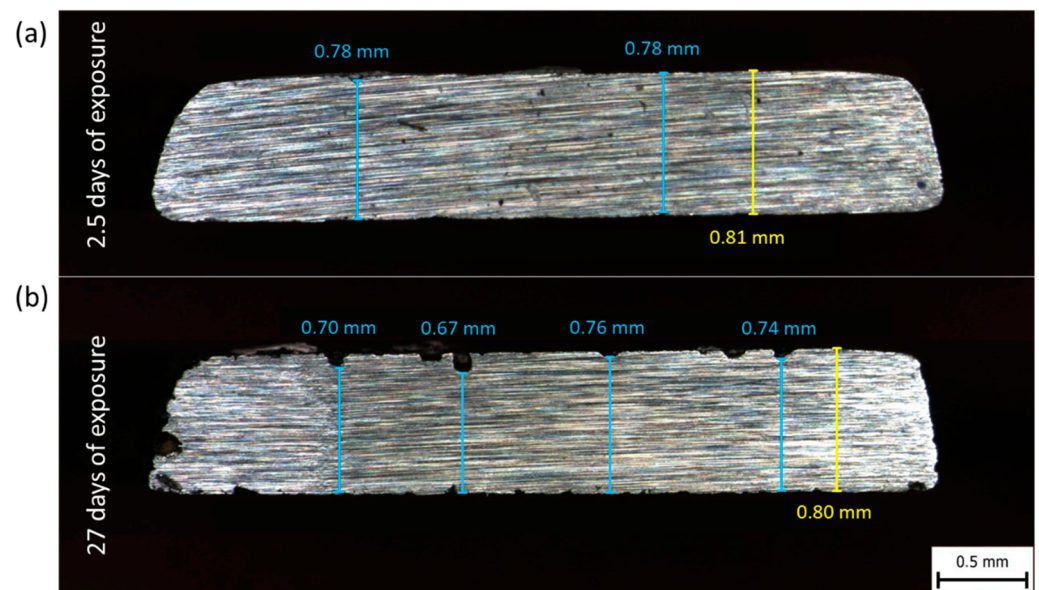


Figure 8. Photographs of cross section of the *Corroding* SSRT specimens with NaCl deposits and exposed in humid air at 85% RH for 2.5 days (a) and 27 days (b).

Pitting can remarkably affect tensile properties of steel. A significant drop in ductility and strength with increasing pits depth was reported [59,60]. When localized corrosion occurs, pits become dominant crack initiation sites, as the stress concentration factor reaches the maximum in the vicinity of pits. Thus, pitting corrosion may have a more harmful effect on the tensile characteristics than general corrosion [61,62] and even change the fracture mode from ductile to brittle. In the current work, the stress concentration induced by pitting probably led to the decrease of elongation and tensile strength with time of exposure of both *Corroding* and *Annealed* specimens.

Sheng et al. [60] showed that a decrease of tensile strength is linked mainly to a cross-sectional area loss. They reported a 20% drop in ultimate load for samples with 19% cross-sectional area loss. In the current work, the cross-sectional area loss evaluated for

the *Corroding* specimen exposed for 27 days (Figure 8) nearby the fracture region was 4%, whereas the tensile strength dropped by 6%. A somewhat higher cross-sectional area loss might be expected in the fracture region as fracture occurs in the region with the highest stress concentration presumably caused by intense pitting.

In contrary, it was demonstrated that elongation is mainly affected by pit depth and density [60]. Jakubowski stated that uniform corrosion does not reduce elongation significantly, while pitting corrosion does [63]. This fits the current observation of 42% loss of elongation as a consequence of 27 days of exposure to corrosive environment accompanied by only 4% cross-sectional area loss. Obviously, corrosion pits served as stress concentrators reducing the elongation significantly.

4. Discussion

It is expected that under conditions of the current study, the effect of pit formation probably overlaid the effect of absorbed hydrogen. It can be assumed that the amount of hydrogen absorbed into the specimens during the exposure did not reach a critical value for the investigated steel. It is known that until reaching a certain minimal hydrogen content in the material, the effect of diffusing hydrogen is negligible and any drop in mechanical properties appears only above such a threshold hydrogen concentration. A longer exposure or more severe exposure conditions could lead to an increased hydrogen entry causing actual hydrogen induced deterioration of mechanical properties. HERS results in Figure 3 show that the longer exposure time of 40 days was indeed linked to a higher hydrogen uptake of 1.1–1.2 ppm. Specimens to be mechanically tested after more than 28 days are currently exposed and obtained results will be given in a follow up paper. On the other hand, higher severity of exposure conditions could enhance pitting. Thus, the effect of corrosion deterioration needs to be carefully considered in such studies in order to avoid any misinterpretation of the role of atomic hydrogen.

There are several works reporting a significant loss of mechanical properties due to hydrogen entry induced by atmospheric corrosion. Li et al. and Akiyama et al. [21,22] reported 55% loss of notch tensile strength after exposure of boron-bearing steel with tensile strength of 1500 MPa to 120 8-h cycles of a cyclic corrosion test (CCT) with a salt spray phase and attributed it to the effect of absorbed hydrogen. The added diffusible hydrogen content was 0.07 ppm, i.e., 10-times less compared to the hydrogen content measured in the current work. An outdoor exposure of NIMS17 steel with tensile strength of 1700 MPa in rural-coastal environment led to 40% loss of ductility, which was linked to presence of 0.2 ppm of absorbed hydrogen [47]. Such a low hydrogen content was achieved after 9-day exposure under the conditions used in the current work. Liu et al. [64] exposed steel specimens from a medium-manganese steel with tensile strength of 1600 MPa to humid air without any chloride pre-deposition and reported 1.6 ppm of absorbed hydrogen after just 3-day exposure, while elongation and tensile strength decreased by 64% and 13%, respectively. In the current work, between 0 and 0.1 ppm hydrogen was detected after 3-day exposure of the specimens with pre-deposited chlorides and the reported drop of mechanical properties seems to be unlikely under these conditions. Although the steels used in the cited works have higher tensile strength, which can cause a higher susceptibility to hydrogen embrittlement, it is questionable if the reported drops in mechanical properties can be linked only to the presence of atomic hydrogen.

In view of the results obtained in this study, it is meaningful to consider whether the degradation of mechanical properties reported in the literature can be attributed entirely to the effect of absorbed hydrogen. The effect of corrosion was not evaluated in these studies although it can be an important factor. Pitting corrosion is very likely in chloride-containing environments and its contribution should be taken into account in such investigations [65]. Li et al. [66] suggested that corrosion-induced reduction of ductility and tensile strength should be considered as the combined effect of several factors, including effect of absorbed hydrogen and stress at corrosion pits.

The aspect of corrosion-induced thinning and formation of stress concentrators in case of localized corrosion is of strong importance for the study of corrosion-induced hydrogen embrittlement. The effect of corrosion on mechanical properties can be easily excluded when specimens are charged in gaseous hydrogen environment [19,20]. However, gaseous charging provides uniform hydrogen absorption into specimens, while hydrogen absorption under natural conditions is highly inhomogeneous. Therefore, results of mechanical testing after gaseous hydrogen charging cannot be fully comparable to those obtained after exposures under atmospheric conditions. The effect of corrosion should thus be separated using reference specimens after hydrogen removal by annealing, as it was shown in the current work. SSRT enables comparing mechanical properties of reference pre-corroded but non-corroding and hydrogen-free specimens with in situ corroding ones. U-bend testing may provide more critical HE conditions due to combination of exposure to corrosive environment with plastic strain [67]. Since the annealing step cannot be included in such tests, it is impossible to separate effects of corrosion and absorbed hydrogen.

SSRT seems to be an appropriate and fair technique for evaluation of HE caused by atmospheric corrosion with respect to parallel effects of corrosion on sample thinning and formation of stress concentrators. The exposure conditions used in this work did not lead to the change of mechanical properties due to absorbed hydrogen. The effect of more severe exposure conditions such as pre-exposure in SO₂-containing atmosphere or under Neutral Salt Spray Test conditions will be studied in further experiments.

5. Conclusions

- Exposure of unstressed DP1000 steel specimens with chloride deposits to humid air led to hydrogen uptake of 0.7 ppm after 27 days.
- Slow strain rate testing of DP1000 specimens with chloride deposits pre-corroded in humid air for up to 27 days revealed a drop in elongation and tensile strength by 42 and 6%, respectively.
- The drop in elongation and tensile strength was linked to a reduction in the cross-sectional area of the specimens due to corrosion and remarkable pitting and formation of stress concentrators.
- The amount of hydrogen absorbed during 27 days of the exposure was insufficient to cause significant change of mechanical properties of DP1000 steel.
- The results clearly demonstrate that cross-section reduction due to corrosion and pit formation cannot be neglected when evaluating the effect of absorbed hydrogen on mechanical properties of specimens exposed to atmospheric corrosion conditions.
- Slow strain rate testing is optimal for determination of the effect of corrosion-induced hydrogen on mechanical properties of steels as annealed reference specimens can be used allowing for separation of the effect of corrosion damage and atomic hydrogen.

Author Contributions: Conceptualization, T.P., D.R. and G.L.; methodology, T.P. and D.R.; validation, G.S.-A., G.L., A.M. and J.F.; formal analysis, T.P.; investigation, D.R., I.T. and G.S.-A.; data curation, A.M., G.L. and J.F.; writing—original draft preparation, D.R.; writing—review and editing, T.P., J.F.; supervision, T.P., J.F. and G.L.; project administration, T.P., G.L., A.M. and J.F.; funding acquisition, T.P. and G.L. All authors have read and agreed to the published version of the manuscript.

Funding: A part of this research was funded by Czech Science Foundation, grant number 17-22586S. The Comet Centre CEST is funded within the framework of COMET—Competence Centres for Excellent Technologies by BMVIT, BMDW as well as the Province of Lower Austria and Upper Austria. The COMET programme is run by FFG (FFG 865864 CEST-K1).

Data Availability Statement: The data used to support the findings of this study are available from the corresponding authors upon reasonable request.

Conflicts of Interest: The authors declare no conflict of interest. The funders had no role in the design of the study; in the collection, analyses, or interpretation of data; in the writing of the manuscript, or in the decision to publish the results.

References

- Schmitt, J.H.; Lung, T. New developments of advanced high-strength steels for automotive applications. *Comptes Rendus Phys.* **2018**, *19*, 641–656. [\[CrossRef\]](#)
- Kuziak, R.; Kawalla, R.; Waengler, S. Advanced high strength steels for automotive industry: A review. *Arch. Civ. Mech. Eng.* **2008**, *8*, 103–117. [\[CrossRef\]](#)
- Fonstein, N. Dual-phase steels. In *Woodhead Publishing Series in Metals and Surface Engineering*; Woodhead Publishing: Sawston, UK, 2017; pp. 169–216. [\[CrossRef\]](#)
- Kalhor, A.; Soleimani, M.; Mirzadeh, H.; Uthaisangasuk, V. A review of recent progress in mechanical and corrosion properties of dual phase steels. *Arch. Civ. Mech. Eng.* **2020**, *20*. [\[CrossRef\]](#)
- Rudomilova, D.; Prosek, T.; Luckeneder, G. Techniques for investigation of hydrogen embrittlement of advanced high strength steels. *Corros. Rev.* **2018**, *36*, 413–434. [\[CrossRef\]](#)
- Rehrl, J.; Mraczek, K.; Pichler, A.; Werner, E. Mechanical properties and fracture behavior of hydrogen charged AHSS/UHSS grades at high- and low strain rate tests. *Mater. Sci. Eng. A Struct.* **2014**, *590*, 360–367. [\[CrossRef\]](#)
- Depover, T.; Escobar, D.P.; Wallaert, E.; Zermout, Z.; Verbeken, K. Effect of hydrogen charging on the mechanical properties of advanced high strength steels. *Int. J. Hydrogen Energy* **2014**, *39*, 4647–4656. [\[CrossRef\]](#)
- Chida, T.; Hagihara, Y.; Akiyama, E.; Iwanaga, K.; Takagi, S.; Hayakawa, M.; Ohishi, H.; Hirakami, D.; Tarui, T. Comparison of Constant Load, SSRT and CSRT Methods for Hydrogen Embrittlement Evaluation Using Round Bar Specimens of High Strength Steels. *ISIJ Int.* **2016**, *56*, 1268–1275. [\[CrossRef\]](#)
- Lovicu, G.; Bottazzi, M.; D'Aiuto, F.; De Sanctis, M.; Dimatteo, A.; Santus, C.; Valentini, R. Hydrogen embrittlement of automotive advanced high-strength steels. *Metall. Mater. Trans. A* **2012**, *43*, 4075–4087. [\[CrossRef\]](#)
- Rehrl, J.; Mraczek, K.; Pichler, A.; Werner, E. The Impact of Nb, Ti, Zr, B, V, and Mo on the Hydrogen Diffusion in Four Different AHSS/UHSS Microstructures. *Steel Res. Int.* **2014**, *85*, 336–346. [\[CrossRef\]](#)
- Vanova, P.; Sojka, J. Hydrogen Embrittlement of Duplex Steel Tested Using Slow Strain Rate Test. *Metalurgija* **2014**, *53*, 163–166.
- Wang, M.; Akiyama, E.; Tsuzaki, K. Effect of hydrogen on the fracture behavior of high strength steel during slow strain rate test. *Corros. Sci.* **2007**, *49*, 4081–4097. [\[CrossRef\]](#)
- Wang, M.Q.; Akiyama, E.; Tsuzaki, K. Fracture criterion for hydrogen embrittlement of high strength steel. *Mater. Sci. Technol. Lond.* **2006**, *22*, 167–172. [\[CrossRef\]](#)
- Depover, T.; Wallaert, E.; Verbeken, K. Fractographic analysis of the role of hydrogen diffusion on the hydrogen embrittlement susceptibility of DP steel. *Mater. Sci. Eng. A Struct.* **2016**, *649*, 201–208. [\[CrossRef\]](#)
- Xu, H.; Xia, X.M.; Hua, L.; Sun, Y.; Dai, Y.L. Evaluation of hydrogen embrittlement susceptibility of temper embrittled 2.25Cr-1Mo steel by SSRT method. *Eng. Fail. Anal.* **2012**, *19*, 43–50. [\[CrossRef\]](#)
- Koyama, M.; Akiyama, E.; Sawaguchi, T.; Raabe, D.; Tsuzaki, K. Hydrogen-induced cracking at grain and twin boundaries in an Fe-Mn-C austenitic steel. *Scr. Mater.* **2012**, *66*, 459–462. [\[CrossRef\]](#)
- Cwiek, J. Hydrogen assisted cracking of high-strength weldable steels in sea-water. *J. Mater. Process. Technol.* **2005**, *164*, 1007–1013. [\[CrossRef\]](#)
- Hu, Y.B.; Dong, C.F.; Luo, H.; Xiao, K.; Zhong, P.; Li, X.G. Study on the Hydrogen Embrittlement of Aermet100 Using Hydrogen Permeation and SSRT Techniques. *Metall. Mater. Trans. A* **2017**, *48*, 4046–4057. [\[CrossRef\]](#)
- Loidl, M.; Kolk, O.; Veith, S.; Gobel, T. Characterization of hydrogen embrittlement in automotive advanced high strength steels. *Materialwissenschaft Werkstofftechnik* **2011**, *42*, 1105–1110. [\[CrossRef\]](#)
- Hejazi, D.; Calka, A.; Dunne, D.; Pereloma, E. Effect of gaseous hydrogen charging on the tensile properties of standard and medium MnX70 pipeline steels. *Mater. Sci. Technol. Lond.* **2016**, *32*, 675–683. [\[CrossRef\]](#)
- Akiyama, E.; Wang, M.Q.; Li, S.J.; Zhang, Z.G.; Kimura, Y.; Uno, N.; Tsuzaki, K. Studies of Evaluation of Hydrogen Embrittlement Property of High-Strength Steels with Consideration of the Effect of Atmospheric Corrosion. *Metall. Mater. Trans. A* **2013**, *44*, 1290–1300. [\[CrossRef\]](#)
- Li, S.J.; Zhang, Z.G.; Akiyama, E.; Tsuzaki, K.; Zhang, B.P. Evaluation of susceptibility of high strength steels to delayed fracture by using cyclic corrosion test and slow strain rate test. *Corros. Sci.* **2010**, *52*, 1660–1667. [\[CrossRef\]](#)
- Birnbaum, H.K.; Sofronis, P. Hydrogen-Enhanced Localized Plasticity—A Mechanism for Hydrogen-Related Fracture. *Mater. Sci. Eng. A Struct.* **1994**, *176*, 191–202. [\[CrossRef\]](#)
- Robertson, I.M. The effect of hydrogen on dislocation dynamics. *Eng. Fract. Mech.* **2001**, *68*, 671–692. [\[CrossRef\]](#)
- Akiyama, E.; Matsukado, K.; Li, S.J.; Tsuzaki, K. Constant-load delayed fracture test of atmospherically corroded high strength steels. *Appl. Surf. Sci.* **2011**, *257*, 8275–8281. [\[CrossRef\]](#)
- Hagihara, Y.; Shobu, T.; Hisamori, N.; Suzuki, H.; Takai, K.; Hirai, K. Delayed Fracture Using CSRT and Hydrogen Trapping Characteristics of V-bearing High-strength Steel. *ISIJ Int.* **2012**, *52*, 298–306. [\[CrossRef\]](#)
- Rudomilova, D.; Petrek, T.; Prosek, T.; Sefl, V.; Duchaczek, H.; Zwettler, F.; Muhr, A.; Luckeneder, G. Comparative study of devices for hydrogen permeation measurements. *Mater. Corros.* **2018**, *69*, 1398–1402. [\[CrossRef\]](#)
- Rudomilova, D.; Prosek, T.; Salvetr, P.; Knaislova, A.; Novak, P.; Kodym, R.; Schimo-Aichhorn, G.; Muhr, A.; Duchaczek, H.; Luckeneder, G. The effect of microstructure on hydrogen permeability of high strength steels. *Mater. Corros.* **2019**. [\[CrossRef\]](#)
- Kirchheim, R.; Gegner, J.; Wilbrandt, P.J. Verfahren zum Nachweis von Wasserstoff in Stahl. EU Patent EP2013616 B1, 21 December 2011.

30. Depover, T.; Vercruyssen, F.; Elmahdy, A.; Verleysen, P.; Verbeken, K. Evaluation of the hydrogen embrittlement susceptibility in DP steel under static and dynamic tensile conditions. *Int. J. Impact Eng.* **2019**, *123*, 118–125. [CrossRef]
31. Nagumo, M.; Nakamura, M.; Takai, K. Hydrogen thermal desorption relevant to delayed-fracture susceptibility of high-strength steels. *Metall. Mater. Trans. A* **2001**, *32*, 339–347. [CrossRef]
32. Sojka, J.; Vodarek, V.; Schindler, I.; Ly, C.; Jerome, M.; Vanova, P.; Ruscassier, N.; Wenglorzova, A. Effect of hydrogen on the properties and fracture characteristics of TRIP 800 steels. *Corros. Sci.* **2011**, *53*, 2575–2581. [CrossRef]
33. Toji, Y.; Takagi, S.; Yoshino, M.; Hasegawa, K.; Tanaka, Y. Evaluation of Hydrogen Embrittlement for High Strength Steel Sheets. *Mater. Sci. Forum* **2010**, *638–642*, 3537–3542. [CrossRef]
34. Takagi, S.; Toji, Y.; Yoshino, M.; Hasegawa, K. Hydrogen Embrittlement Resistance Evaluation of Ultra High Strength Steel Sheets for Automobiles. *ISIJ Int.* **2012**, *52*, 316–322. [CrossRef]
35. Kinugasa, J.; Yuse, F.; Tsunazawa, M.; Nakaya, M. Effect of Corrosion Resistance and Rust Characterization for Hydrogen Absorption into Steel under an Atmospheric Corrosion Condition. *ISIJ Int.* **2016**, *56*, 459–464. [CrossRef]
36. Akiyama, E.; Li, S.J.; Shinohara, T.; Zhang, Z.G.; Tsuzaki, K. Hydrogen entry into Fe and high strength steels under simulated atmospheric corrosion. *Electrochim. Acta* **2011**, *56*, 1799–1805. [CrossRef]
37. Ajito, S.; Tada, E.; Ooi, A.; Nishikata, A. Simultaneous Measurements of Corrosion Potential and Hydrogen Permeation Current in Atmospheric Corrosion of Steel. *ISIJ Int.* **2019**, *59*, 1659–1666. [CrossRef]
38. Dual-Phase Steels Voestalpine EN 12062019. Available online: <https://www.voestalpine.com/ultralights/en/content/download/4523/file/Dual-phase-steels-voestalpine-EN-12062019.pdf> (accessed on 21 December 2020).
39. Knaislová, A.; Rudomilova, D.; Novák, P.; Prošek, T.; Michalcová, A.; Beran, P. Critical Assessment of Techniques for the Description of the Phase Composition of Advanced High-Strength Steels. *Materials* **2019**, *12*, 4033. [CrossRef]
40. Prosek, T.; Thierry, D.; Taxen, C.; Maixner, J. Effect of cations on corrosion of zinc and carbon steel covered with chloride deposits under atmospheric conditions. *Corros. Sci.* **2007**, *49*, 2676–2693. [CrossRef]
41. Cole, I.S.; Neufeld, A.K.; Furman, S.; Miao, W.; Sherman, N. Response of 55% aluminium-zinc coated steel and zinc to well-defined salt doses under controlled environments. In *The Electrochemical Society Proceedings*; IOP Science: Bristol, UK, 2000; Volume 2000-23.
42. Kreislova, K.; Geiplova, H.; Lanik, T.; Hovorkova, K. The effect of road environment on corrosion of the infrastructure constructions. In *Proceedings of the Eurocorr 2011, Stockholm, Sweden, 4–8 September 2011*; Eurocorr: Frankfurt, Germany, 2011.
43. Takai, K.; Shoda, H.; Suzuki, H.; Nagumo, M. Lattice defects dominating hydrogen-related failure of metals. *Acta Mater.* **2008**, *56*, 5158–5167. [CrossRef]
44. Zhou, C.S.; Ye, B.G.; Song, Y.Y.; Cui, T.C.; Xu, P.; Zhang, L. Effects of internal hydrogen and surface-absorbed hydrogen on the hydrogen embrittlement of X80 pipeline steel. *Int. J. Hydrogen Energy* **2019**, *44*, 22547–22558. [CrossRef]
45. Ajito, S.; Tada, E.; Ooi, A.; Nishikata, A. Hydrogen Absorption Behavior of Pre-Rusted Steels under a NaCl Droplet. *J. Electrochem. Soc.* **2019**, *166*, C243–C249. [CrossRef]
46. Akiyama, E.; Matsukado, K.; Wang, M.Q.; Tsuzaki, K. Evaluation of hydrogen entry into high strength steel under atmospheric corrosion. *Corros. Sci.* **2010**, *52*, 2758–2765. [CrossRef]
47. Li, S.J.; Akiyama, E.; Yuuji, K.; Tsuzaki, K.; Uno, N.; Zhang, B.P. Hydrogen embrittlement property of a 1700-MPa-class ultrahigh-strength tempered martensitic steel. *Sci. Technol. Adv. Mater.* **2010**, *11*. [CrossRef] [PubMed]
48. Ronevich, J.A.; Speer, J.G.; Matlock, D.K. Hydrogen embrittlement of commercially produced advanced high strength sheet steels. *SAE Int. J. Mater. Manuf.* **2010**, *3*, 255–267. [CrossRef]
49. Alp, T.; Dogan, B.; Davies, T.J. The Effect of Microstructure in the Hydrogen Embrittlement of a Gas-Pipeline Steel. *J. Mater. Sci.* **1987**, *22*, 2105–2112. [CrossRef]
50. Liu, Q.; Atrens, A. A critical review of the influence of hydrogen on the mechanical properties of medium-strength steels. *Corros. Rev.* **2013**, *31*, 85–103. [CrossRef]
51. Zhang, J.; Li, X.Y.; Rong, L.J.; Li, Y.Y. Effect of hydrogen on internal friction of a FE-BASED austenitic alloy. *Aip Conf. Proc.* **2008**, *986*, 10–17.
52. Marchi, C.S.; Somerday, B.P.; Tang, X.; Schiroky, G.H. Effects of alloy composition and strain hardening on tensile fracture of hydrogen-precharged type 316 stainless steels. *Int. J. Hydrogen Energy* **2008**, *33*, 889–904. [CrossRef]
53. Lynch, S.; Ryan, N. *Mechanisms of Hydrogen Embrittlement-Crack Growth in a Low-Alloy Ultra-High-Strength Steel Under Cyclic and Sustained Stresses in Gaseous Hydrogen*; Aeronautical Research Labs: Melbourne, Australia, 1978.
54. Lynch, S. Progress towards understanding mechanisms of hydrogen embrittlement and stress corrosion cracking. In *Proceedings of the CORROSION, Nashville, TN, USA, 11–15 March 2007*; Eurocorr: Frankfurt, Germany, 2007.
55. Thompson, A.W. Ductile Fracture Topography—Geometrical Contributions and Effects of Hydrogen. *Metall. Trans. A* **1979**, *10*, 727–731. [CrossRef]
56. Kushida, T. Hydrogen entry into steel by atmospheric corrosion. *ISIJ Int.* **2003**, *43*, 470–474. [CrossRef]
57. Li, S.X.; Hihara, L.H. The comparison of the corrosion of ultrapure iron and low-carbon steel under NaCl-electrolyte droplets. *Corros. Sci.* **2016**, *108*, 200–204. [CrossRef]
58. Defrancq, J.N. Research on Causes of Pitting Corrosion of Low-Carbon Steel. *Corros. Sci.* **1974**, *14*, 461–465. [CrossRef]

59. Xu, S.H.; Wang, H.; Li, A.B.; Wang, Y.D.; Su, L. Effects of corrosion on surface characterization and mechanical properties of butt-welded joints. *J. Constr. Steel Res.* **2016**, *126*, 50–62. [[CrossRef](#)]
60. Sheng, J.; Xia, J.W. Effect of simulated pitting corrosion on the tensile properties of steel. *Constr. Build. Mater.* **2017**, *131*, 90–100. [[CrossRef](#)]
61. Zhao, Z.W.; Zhang, H.W.; Xian, L.N.; Liu, H.Q. Tensile strength of Q345 steel with random pitting corrosion based on numerical analysis. *Thin Wall Struct.* **2020**, *148*. [[CrossRef](#)]
62. Nakai, T.; Matsushita, H.; Yamamoto, N.; Arai, H. Effect of pitting corrosion on local strength of hold frames of bulk carriers (1st report). *Mar. Struct.* **2004**, *17*, 403–432. [[CrossRef](#)]
63. Jakubowski, M. Influence of pitting corrosion on strength of steel ships and offshore structures. *Pol. Marit. Res.* **2011**, *18*, 54–58. [[CrossRef](#)]
64. Liu, Q.Y.; Xu, J.P.; Shen, L.C.; Zhou, Q.J.; Su, Y.J.; Qiao, L.J.; Yan, Y. Effect of Relative Humidity on Mechanical Degradation of Medium Mn Steels. *Materials* **2020**, *13*, 1304. [[CrossRef](#)]
65. Wasim, M.; Li, C.Q.; Mahmoodian, M.; Robert, D. Mechanical and Microstructural Evaluation of Corrosion and Hydrogen-Induced Degradation of Steel. *J. Mater. Civ. Eng.* **2019**, *31*. [[CrossRef](#)]
66. Li, L.; Mahmoodian, M.; Li, C.Q.; Robert, D. Effect of corrosion and hydrogen embrittlement on microstructure and mechanical properties of mild steel. *Constr. Build. Mater.* **2018**, *170*, 78–90. [[CrossRef](#)]
67. Kim, H.-J.; Lee, M.-G.; Yoon, S.-C.; Vucko, F.; Lee, C.-W.; Theiry, D.; Kim, S.-J. Diffusible hydrogen behavior and delayed fracture of cold rolled martensitic steel in consideration of automotive manufacturing process and vehicle service environment. *J. Mater. Res. Technol.* **2020**, *9*, 13483–13501. [[CrossRef](#)]